Spectrochimica Acta Part A: Molecular and Biomolecular Spectroscopy 115 (2013) 399–408

Contents lists available at SciVerse ScienceDirect

Spectrochimica Acta Part A: Molecular and Biomolecular Spectroscopy

journal homepage: www.elsevier.com/locate/saa

Binary and ternary copper(II) complexes of a tridentate ONS ligand derived from 2-aminochromone-3 carboxaldehyde and thiosemicarbazide: Synthesis, spectral studies and antimicrobial activity

Magdy Shebl *, M.A. Ibrahim, Saied M.E. Khalil, S.L. Stefan, H. Habib

Department of Chemistry, Faculty of Education, Ain Shams University, Roxy, Cairo, Egypt

HIGHLIGHTS

- A tridentate thiosemicarbazone ligand was synthesized.
- Copper(II) complexes were synthesized and characterized by analytical and spectral methods.
- The spin Hamiltonian parameters of some complexes were calculated and discussed.
- The ligand and some Cu(II) complexes showed antimicrobial activity.

GRAPHICAL ABSTRACT

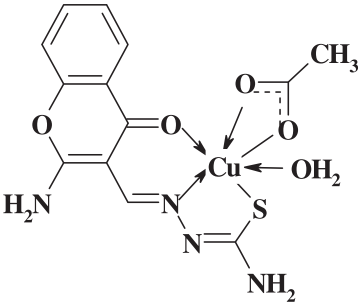

[(L)Cu(OAc)(H$_2$O)]

ARTICLE INFO

Article history:
Received 15 March 2013
Received in revised form 12 June 2013
Accepted 19 June 2013
Available online 1 July 2013

Keywords:
Thiosemicarbazones
2-Aminochromone-3-carboxaldehyde
Tridentate ligands
EPR spectra
Binary and ternary complexes
Antimicrobial activity

ABSTRACT

A tridentate ONS donor ligand, HL, was synthesized by the condensation of 2-aminochromone-3-carboxaldehyde with thiosemicarbazide. The structure of the ligand was elucidated by elemental analyses, IR, ^{1}H and ^{13}C NMR, electronic and mass spectra. Reaction of the ligand with several copper(II) salts, including AcO$^-$, NO_3^-, SO_4^{2-}, Cl$^-$, Br$^-$ and ClO_4^- afforded different metal complexes that reflect the non-coordinating or weakly coordinating power of the ClO_4^- and Br$^-$ anions as compared to the strongly coordinating power of AcO$^-$, SO_4^{2-}, Cl$^-$ and NO_3^- anions. Also, the ligand was allowed to react with Cu(II) ion in the presence of a secondary ligand (L′) [N,O-donor; 8-hydroxyquinoline or N,N-donor; 1,10-phenanthroline]. Characterization and structure elucidation of the prepared complexes were achieved by elemental and thermal analyses, IR, electronic, mass and EPR spectra as well as conductivity and magnetic susceptibility measurements. The EPR spin Hamiltonian parameters of some complexes were calculated. The metal complexes exhibited octahedral and square planar geometrical arrangements depending on the nature of the anion. The ligand and most of its metal complexes showed antibacterial activity towards Gram-positive bacteria (*Staphylococcus aureus* and *Bacillus subtilis*), Gram-negative bacteria (*Salmonella typhimurium* and *Escherichia coli*), yeast (*Candida albicans*) and fungus (*Aspergillus fumigatus*).

Introduction

Because of their simple preparation, excellent complexation of not only transition but also non-transition p-block elements, interesting structural characteristics of their complexes, along with the possibility of their analytical application, thiosemicarbazones have become a subject of intense research interest of coordination chemists. This has resulted in a large number of papers and several reviews [1,2] that summarized various aspects of the chemistry of these compounds, such as methods of their synthesis, spectral, magnetic, stereochemical, structural and other characteristics. An

---

* Corresponding author. Tel.: +20 233120546.
E-mail address: magdy_shebl@hotmail.com (M. Shebl).

1386-1425/$ - see front matter
http://dx.doi.org/10.1016/j.saa.2013.06.075

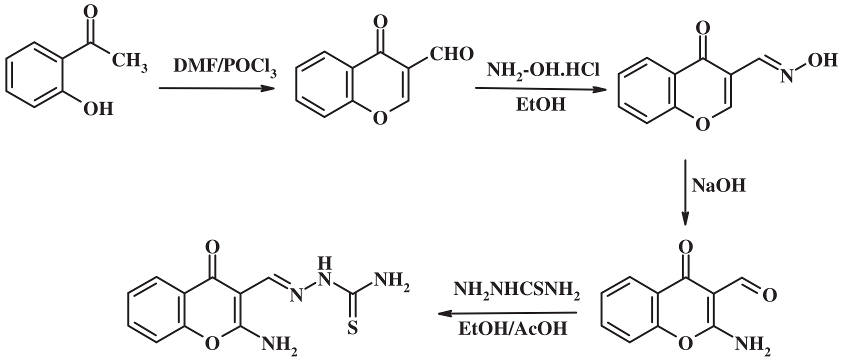

Scheme 1. The synthetic pathway for the ligand.

Table 1
Analytical and physical data of the thiosemicarbazone, HL, ligand and its complexes.

No.	Reaction	Complex M. F. [F. Wt]	Color	Yield (%)	M.P. °C	Elemental analysis, % Found/(Calc.)				
						C	H	N	Cl/S	M
	HL	$C_{11}H_{10}O_2N_4S$ [262.29]	Yellow	73	>300	50.35 50.37	3.83 3.84	21.14 (21.36)	12.04 (12.22)	–
(1)	HL + $Cu(OAc)_2{\cdot}H_2O$	$[(L)Cu(OAc)(H_2O)]$ $C_{13}H_{14}N_4O_5SCu$ [401.89]	Brown	64	269	39.0 (38.85)	3.10 (3.51)	14.2 (13.94)	8.20 (7.98)	15.7 (15.81)
(2)	HL + $Cu(NO_3)_2{\cdot}2.5H_2O$	$[(L)Cu(NO_3)]$ $C_{11}H_9N_5O_5SCu$ [386.83]	Green	59	244	34.30 (34.16)	2.60 (2.35)	17.80 (18.10)	8.00 (8.29)	16.10 (16.43)
(3)	HL + $CuSO_4{\cdot}5H_2O$	$[(HL)Cu(SO_4)(H_2O)]$ $C_{11}H_{12}N_4O_7S_2Cu$ [439.91]	Green	57	279	29.97 (30.03)	3.0 (2.75)	12.30 (12.75)	14.10 (14.58)	14.30 (14.45)
(4)	HL + $Cu(ClO_4)_2{\cdot}6H_2O$	$[(HL)Cu(H_2O)_3](ClO_4)_2{\cdot}3H_2O$ $C_{11}H_{22}N_4O_{16}SCu$ [632.83]	Green	62	–[a]	20.85 (20.88)	3.49 (3.50)	8.6 (8.85)	11.10/5.20 (11.20)/(5.07)	9.90 (10.04)
(5)	HL + $CuCl_2{\cdot}2H_2O$	$[(L)CuCl(H_2O)]{\cdot}0.5H_2O$ $C_{11}H_{10}N_4O_{2.5}SClCu$ [369.29]	Green	82	271	35.40 (35.78)	2.50 (2.73)	15.40 (15.17)	9.80/8.50 (9.60)(8.68)	17.10 (17.21)
(6)	HL + $CuBr_2$	$[(L)Cu(H_2O)]Br$ $C_{11}H_{11}N_4O_3SBrCu$ [422.75]	Green	91	266	31.00 (31.25)	2.63 (2.62)	13.10 (13.25)	7.40 (7.58)	15.00 (15.03)
(7)	HL + $Cu(NO_3)_2{\cdot}2.5H_2O$ + 8-HQ	$[(L)Cu(8\text{-}HQ)(H_2O)]$ $C_{20}H_{17}N_5O_4SCu$ [487.00]	Green	64	>300	49.70 (49.33)	3.38 (3.52)	14.00 (14.38)	6.20 (6.58)	12.90 (13.05)
(8)	HL + $Cu(NO_3)_2{\cdot}2.5H_2O$ + Phen	$[(L)Cu(NO_3)(Phen)]$ $C_{23}H_{17}N_7O_5SCu$ [567.05]	Green	58	274	48.89 (48.72)	3.33 (3.02)	17.00 (17.29)	5.30 (5.65)	11.40 (11.21)

[a] Not determined.

Table 2
Characteristic IR spectral data of the HL ligand and its complexes.

No.	Complex	IR Spectra $(cm)^{-1}$							
		$\nu(NH_2, NH)$	$\nu(C{=}O)$	$\nu(C{=}N)$	$\nu(C{=}C)$	$\nu(C{=}S)$	$\nu(M{-}O)$	$\nu(M{-}N)$	Other bands
	HL	3333, 3279	1644	1558	1519	1331	–	–	
1	$[(L)Cu(OAc)(H_2O)]$	3340, 3269	1605	1550	1517	–	522	447	1404 $\nu_{as}(COO^-)$, 1335 $\nu_s(COO^-)$; (bidentate OAc^-)
2	$[(L)Cu(NO_3)]$	3317, 3282	1639	1549	1457	–	470	430	1366, 1159; $\nu(NO_3^-)$ (monodentate)
3	$[(HL)Cu(SO_4)(H_2O)]$	3407, 3276	1619	1548	1510	1300	507	461	1167, 1019; $\nu(SO_4^{2-})$ (bidentate)
4	$[(HL)Cu(H_2O)_3](ClO_4)_2{\cdot}3H_2O$	3417, 3319	1616	1537	1510	1322	500	458	1089, 625; $\nu(ClO_4^-)$ (ionic)
5	$[(L)CuCl(H_2O)]{\cdot}0.5H_2O$	3334, 3285	1621	1530	1487	–	513	436	
6	$[(L)Cu(H_2O)]Br$	3347, 3275	1620	1540	1488	–	511	430	
7	$[(L)Cu(8\text{-}HQ)(H_2O)]$	3224, 3150	1608	1546	1473	–	470	428	
8	$[(L)Cu(NO_3)(Phen)]$	3430, 2970	1607	1550	1520	–	503	430	1404, 1138; $\nu(NO_3^-)$ (monodentate)

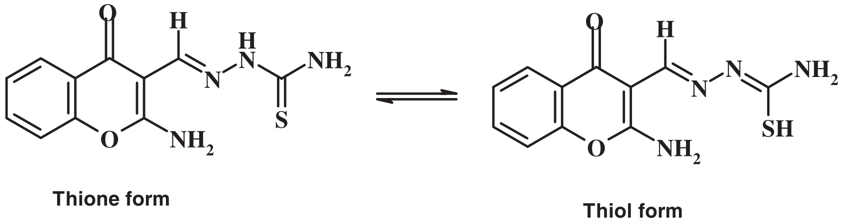

Scheme 2. Tautomeric forms of the ligand.

Table 3
Electronic spectra, magnetic moments and molar conductivity data of the HL ligand and its complexes.

No.	Complex	Electronic spectral bands[a] (nm) λ_{max}[a] (nm)/(ε_{max} L cm^{-1} mol^{-1})	$\mu_{eff.}$ B.M.	Conductance[a] (Ω^{-1} cm^2 mol^{-1})
	HL	292 (3600), 356 (3900), 428 (3300)	–	–
1	$[(L)Cu(OAc)(H_2O)]$	(472, 665)[b]	1.63	5.95
2	$[(L)Cu(NO_3)]$	(576)[b]	1.54	5.00
3	$[(HL)Cu(SO_4)(H_2O)]$	(486, 592)[b]	1.78	27.1
4	$[(HL)Cu(H_2O)_3](ClO_4)_2\cdot 3H_2O$	(480, 625)[c]	1.45	130
5	$[(L)CuCl(H_2O)]\cdot 0.5H_2O$	(582)[b]	1.58	29.3
6	$[(L)Cu(H_2O)]Br$	(573)[c]	1.56	105
7	$[(L)Cu(8\text{-}HQ)(H_2O)]$	(455, 620)[b]	1.65	9.29
8	$[(L)Cu(NO_3)(Phen)]$	(465,578)[b]	1.66	23.2

[a] Solutions in DMF (10^{-3} M).
[b] Nujol mull.
[c] Concentrated solutions.

Table 4
^{1}H NMR spectral data of the HL ligand.

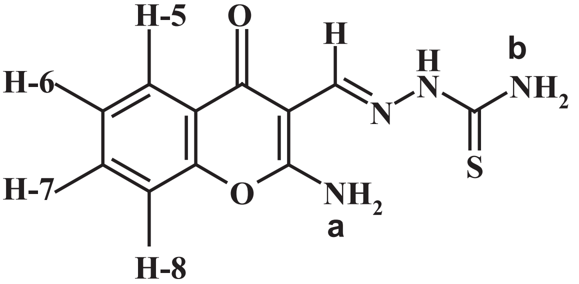

Chemical shifts in ppm (DMSO)	Assignment
7.38–7.44	(m, 2H, H-6 and H-8)
7.69	(t, 1H, H-7, J = 8.2 Hz)
7.9	(br, 1H, NH, exchangeable with D_2O)
7.99	(d, 1H, H-5, J = 8.2 Hz)
8.64	(br, 3H, CH=N and NH_2(a))
11.08	(br, 2H, NH_2 (b) exchangeable with D_2O)

Table 5
^{13}C NMR spectral data of the HL ligand.

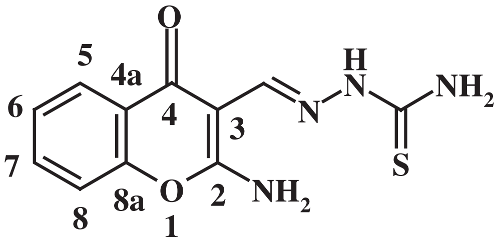

Chemical shifts in ppm (DMSO)	Assignment
91.8	C-3
116.4	C-8
121.4	CH=N
124.8	C-4a
125.1	C-6
133	C-7
142.2	C-5
152.5	C-8a
161.8	C-2
173.4	C=S
176.2	C-4 as C=O

enhanced interest in these compounds has aroused the discovery of their beneficial pharmacological properties such as antiviral, antibacterial and antitumoral activities [3–10]. Also, compounds contain in their structure chromone ring have attracted attention because of their interesting biological properties. Many of them show antimicrobial, antiallergic, antiviral, antihypertensive, anticancer and antioxidant activities [11–17]. The present study, is an extension to our work including thiosemicarbazone complexes [18–21], and aims to study the ligational behavior of a new thiosemicarbazone ligand, obtained from the condensation of thiosemicarbazide and 2-aminochromone-3-carboxaldehyde, towards copper(II) ion. A series of binary and ternary complexes have been synthesized and characterized by elemental and thermal analyses, IR, electronic, EPR and mass spectra as well as conductivity and magnetic susceptibility measurements at room temperature. The biological activity of the ligand and its complexes was screened against selected kinds of bacteria and fungi.

Experimental

Materials

Metal salts, 2-hydroxyacetophenone, phosphorus oxychloride, hydroxylamine hydrochloride, thiosemicarbazide, were either Aldrich, BDH or Merck products. 3-Formylchromone [22], 2-aminochromone-3-carboxaldehyde [23], 2-aminochromone-3-carboxaldehyde-thiosemicarbazone [24] were prepared according to literature. 8-Hydroxyquinoline, 1,10-phenanthroline, EDTA disodium salt, ammonium hydroxide, mureoxide and nitric acid were either BDH or Merck products. Organic solvents (methanol, absolute ethanol, diethylether, dimethylformamide (DMF) and dimethylsulfoxide (DMSO)) were reagent grade chemicals and were used without further purification.

Caution! Perchlorate compounds of metal ions are potentially explosive especially in the presence of organic ligands. Only a small amount should be prepared and handled with care.

Measurements

Elemental analyses (C, H, N, S and Cl) were carried out at the National Research Center, Dokki, Giza, Egypt. Analysis of the copper(II) ion followed the dissolution of the solid complex in concentrated HNO_3, neutralizing the diluted aqueous solutions with ammonia and titrating the metal solutions with EDTA. Melting points of the complexes were determined using a Stuart SMP3 melting point apparatus. The FT-IR spectra (4000–400 cm^{-1}) were recorded as KBr discs using FT-IR-4000 (Shimadzu) spectrophotometer. The electronic spectra were recorded at room temperature on a Jasco model V-550 UV/Vis spectrophotometer as Nujol mulls and/or solutions in DMF. The ^{1}H and ^{13}C NMR spectra were recorded using a Mercury-300BB (300 MHz). Dimethylsulphoxide,

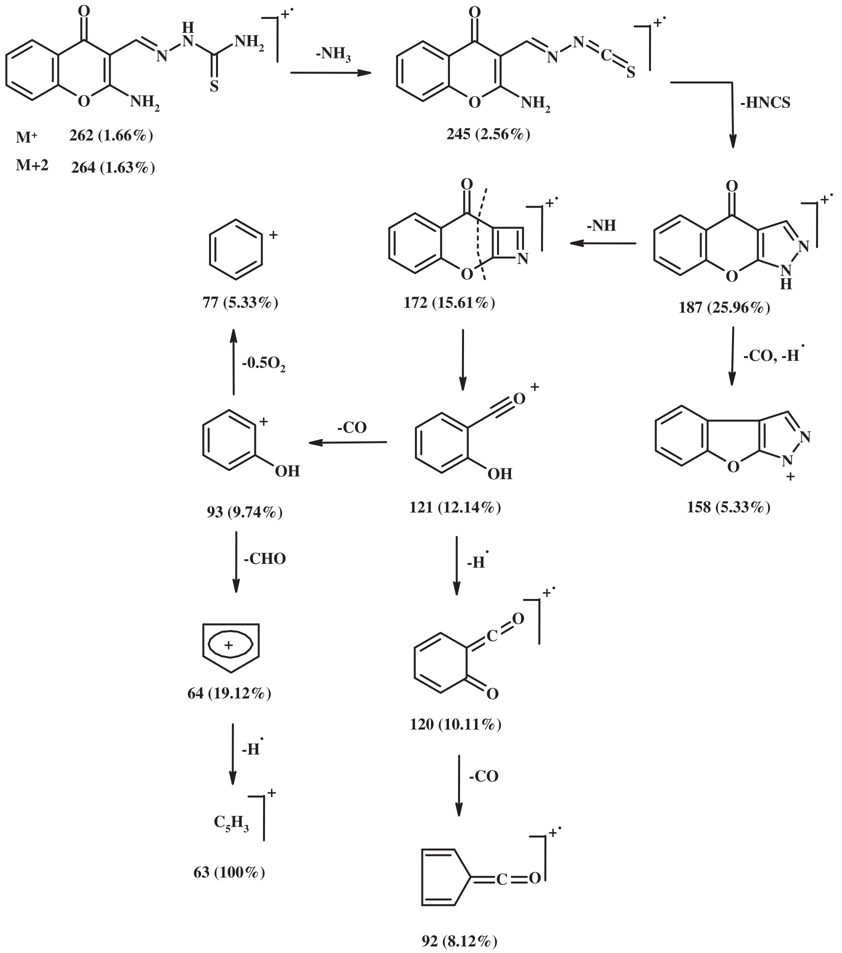

Scheme 3. Mass fragmentation pattern of the ligand.

DMSO-d_6, was used as a solvent and tetramethylsilane (TMS) as an internal reference. EPR spectra of the complexes were recorded at Elexsys, E500, Bruker company. The magnetic field was calibrated with a 2,2′-diphenyl-1-picrylhydrazyl (DPPH) sample purchased from Aldrich. Mass spectra were recorded on GC-2010 Shimadzu Gas chromatography instrument mass spectrometer. Samples were introduced directly to the probe, and the fragmentations were carried out at 300 °C and 70 eV. The magnetic susceptibility measurements were carried out at room temperature using a magnetic susceptibility balance of the type Johnson Matthey, Alfa product, Model No. (MKI). Effective magnetic moments were calculated and corrected using Pascal's constants for the diamagnetism of all atoms in the compounds [25]. Molar conductivities of 10^{-3} M solutions of the solid complexes in DMF were measured on the Corning conductivity meter NY 14831 model 441. TGA-measurements were carried out from room temperature up to 800 °C at a heating rate of 10 °C/min on a Shimadzu-50 thermal analyzer. The biological activity of the ligand and its metal complexes was studied using the disc diffusion method [26].

Synthesis of the thiosemicarbazone ligand, HL

The synthetic steps for the thiosemicarbazone ligand are given in details in Scheme 1. The reaction occurs *via* preparation of 3-formylchromone [22] followed by condensation with hydroxylamine hydrochloride with concomitant rearrangement to produce 2-aminochromone-3-carboxaldehyde [23]. Condensation of the latter compound with thiosemicarbazide afforded the target thiosemicarbazone (HL) ligand [24].

Synthesis of the metal complexes

The metal salt and the ligand, both dissolved in methanol, were mixed in the molar ratio 1:1 (L:M) and refluxed for 5 h. The resulting precipitates were filtered, washed with methanol then ether and finally air-dried. The complexes were kept in a desiccator over anhydrous calcium chloride. The following detailed preparations are given as examples and the other complexes were obtained similarly.

*Synthesis of the [(L)Cu(NO$_3$)], complex (**2**)*

0.7 g (3.0 mmol) of $Cu(NO_3)_2 \cdot 2.5H_2O$ dissolved in 30 mL methanol was added gradually to 0.79 g (3.0 mmol) of the ligand, HL, dissolved in 30 mL methanol. The reaction mixture was refluxed for 5 h which resulted a green precipitate that was filtered off, washed several times with methanol, diethylether and finally air-dried. The yield was 0.685 g (59%).

*Synthesis of [(L)Cu(8-HQ)(H$_2$O)], complex (**7**)*

0.7 g (3.0 mmol) of $Cu(NO_3)_2 \cdot 2.5H_2O$ dissolved in 30 mL methanol was added gradually to 0.79 g (3.0 mmol) of the ligand, HL, dissolved in 30 mL methanol. The reaction mixture was refluxed for 30 min. and then 0.44 g (3.0 mmol) of 8-hydroxyquinoline (8-HQ) dissolved in methanol was added to the above mixture.

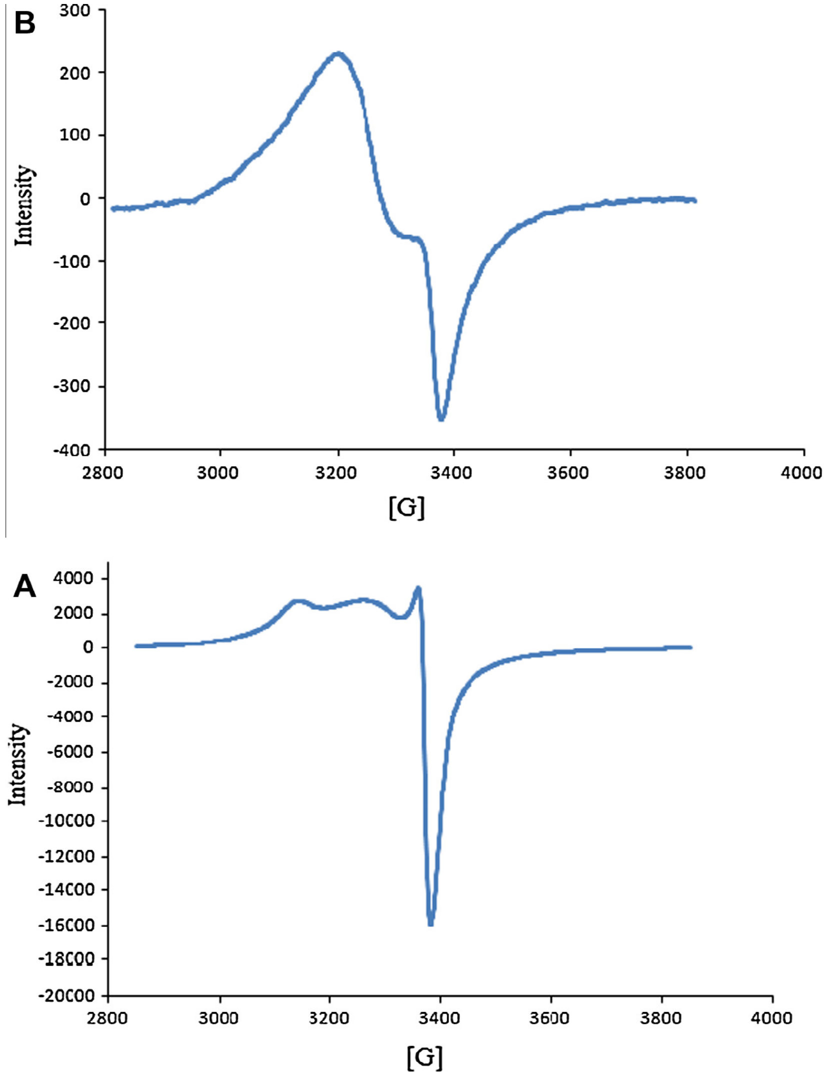

Fig. 1. X-band EPR spectra of the complexes A: $[(HL)Cu(H_2O)_3](ClO_4)_2{\cdot}3H_2O$ (**4**) and B: $[(L)Cu(8\text{-}HQ)(H_2O)]$ (**7**).

Table 6
EPR data of some copper(II) complexes at room temperature.

Complex	$g_{\parallel}$	$g_{\perp}$	$A_{\parallel} \times 10^{-4}$ (cm^{-1})	G	α^2	β^2
$[(HL)Cu(H_2O)_3](ClO_4)_2{\cdot}3H_2O$ (**4**)	2.19	2.06	125	3.17	0.60	0.76
$[(L)Cu(8\text{-}HQ)(H_2O)]$ (**7**)	2.21	2.07	121	3.00	0.61	0.83

The resulting mixture was refluxed for 5 h which resulted a green precipitate that was filtered off, washed several times with methanol, diethylether and finally air-dried. The yield was 0.94 g (64%).

Unsuccessful trials

Trials to prepare ternary Cu(II) complex of HL ligand in the presence of oxalic acid were unsuccessful where the binary complex was obtained.

Antimicrobial activity

The standardized disc-agar diffusion method [26] was followed to determine the activity of the synthesized compounds against the sensitive organisms *Staphylococcus aureus* (ATCC 25923) and *Bacillus subtilis* (ATCC 6635) as Gram positive bacteria, *Salmonella typhimurium* (ATCC 14028) and *Escherichia coli* (ATCC 25922) as Gram negative bacteria and *Candida albicans* (ATCC 10231) and *Aspergillus fumigatus* as fungus strain. The antibiotic chloramphenicol was used as reference in the case of Gram-positive bacteria, cephalothin in the case of Gram-negative bacteria and cycloheximide in the case of fungi.

The compounds were dissolved in DMF which has no inhibition activity to get concentrations of 100 μg mL^{-1} and 50 μg mL^{-1}. The test was performed on medium potato dextrose agars (PDA) which contain infusion of 200 g potatoes, 6 g dextrose and 15 g agar [27]. Uniform size filter paper disks (3 disks per compound) were impregnated by equal volume (10 μL) from the specific concentration of dissolved tested compounds and carefully placed on inoculated agar surface. After incubation for 36 h at 27 °C in the case of bacteria and for 48 h at 24 °C in the case of fungi, inhibition of the organisms was measured and used to calculate mean of inhibition zones.

Results and discussion

Characterization of the ligand

The structure of the ligand was elucidated by elemental analyses, electronic, IR, ^1H and ^{13}C NMR and mass spectra. The results of

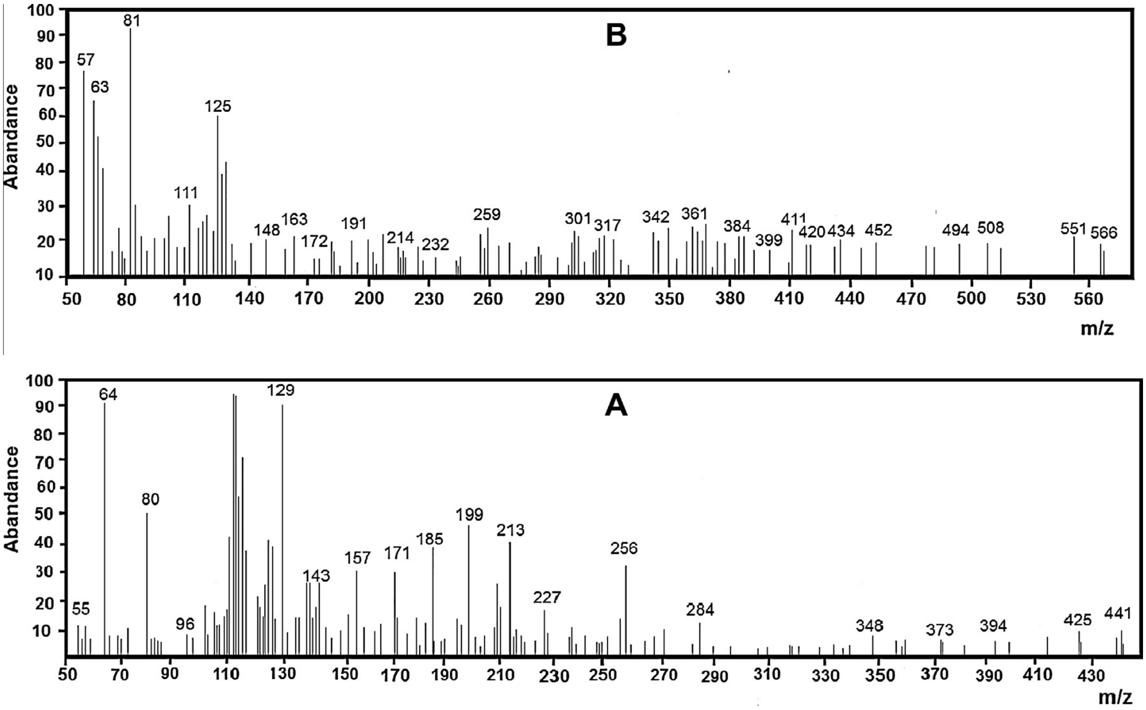

Fig. 2. Mass spectra of the complexes A: [(HL)Cu(SO_4)(H_2O)] (**3**) and B: [(L)Cu(NO_3)(Phen)] (**8**).

the elemental analyses (Table 1) are in good agreement with the proposed formula. The IR spectral data of the ligand (Table 2) showed characteristic absorption bands at 3333, 3279 cm^{-1} assigned to $\nu(2NH_2)$ and ν(NH). The absorption bands observed at 1644, 1558 and 1331 cm^{-1} may be attributed to $\nu(C{=}O_{\gamma\text{-pyrone}})$, ν(C=N) [28,29] and ν(C=S), respectively. The appearance of the latter band, ν(C=S), indicates the existence of the ligand in the solid state in the thione form (Scheme 2). The thionic nature of the ligand is further supported by the absence of an IR band around 2600 cm^{-1} due to ν(SH) [20]. The electronic spectral data of the ligand in DMF (Table 3) showed three bands at 292, 356 and 428 nm. The higher energy band may be assigned to π-π^* transitions of the azomethine linkage and the aromatic benzene ring. The medium energy band may be assigned to n-π^* transitions of the C=O, C=N and C=S groups. Finally, the lower energy band may be attributed to charge transfer (CT) transitions within the molecule. ^1H and ^{13}C NMR spectral data (δ ppm) of the ligand relative to TMS (0 ppm) in DMSO-d_6, Tables 4 and 5, give further support of the suggested structure of the ligand. Moreover, the structure of the ligand was deduced from mass spectral data which showed the molecular ion peak at 262 a.m.u., confirming its formula weight (F.W. 262.29). The mass fragmentation pattern, shown in Scheme 3, supported the suggested structure of the ligand.

Characterization of the metal complexes

The thiosemicarbazone ligand was allowed to react with several Cu(II) salts of AcO^-, NO_3^-, SO_4^{2-}, Cl^-, Br^- and ClO_4^- in order to determine the effect of the counterions on the products. Also, the ligand was allowed to react with copper(II) ion in the presence of secondary ligands (L′) [N,O-donor; 8-hydroxyquinoline or N,N-donor; 1,10-phenanthroline]. The prepared complexes are stable at room temperature, non-hygroscopic and insoluble in water and common organic solvents. The obtained complexes are characterized by elemental and thermal analyses, IR, electronic, EPR and mass spectra as well as conductivity and magnetic measurements.

IR spectra

The IR spectral data of the complexes are listed in Table 2. Comparison of the IR spectra of the metal complexes with that of the free ligand revealed that all complexes (except **2** and **8**) showed a broad band in the range 3410–3456 cm^{-1} assignable to ν(OH) of the coordinated or uncoordinated water molecules associated with the complexes which are confirmed by elemental and thermal analyses. Also, the bands at 1644 and 1558 cm^{-1} assigned to ν(C=O) and ν(C=N), respectively in the free ligand was shifted to lower wave number in all of the complexes, indicating the participation of the γ-pyrone oxygen and azomethine nitrogen in chelation. The band at 1331 cm^{-1} assigned to ν(C=S) in the free ligand was shifted to (1300–1322) cm^{-1} in case of complexes (**3** and **4**) indicating that the coordination occurs through the thione form of the ligand (Scheme 2) [30,31]. However, in other complexes the disappearance of this band provides an evidence that the thiolic S participates in chelation after deprotonation [28]. In complex **1**, the chelating bidentate CH_3COO^- group was supported by bands located at 1404 and 1335 cm^{-1}. These two bands are due to $\nu_{as}(COO^-)$ and $\nu_s(COO^-)$, respectively. The separation of the two bands, $\Delta\nu = (\nu_{as}-\nu_s) = 69\ cm^{-1}$, is comparable to the values cited for the bidentate character of the acetate group [32]; $\Delta\nu = 75$–$80\ cm^{-1}$. The complexes (**2** and **8**) showed bands at 1366 and 1159 cm^{-1}, for the former complex (**2**) and at 1404 and 1138 cm^{-1}, for the latter complex (**8**), indicating the monodentate nature of the coordinated NO_3^- group [33,34]. In complex **3**, the chelating bidentate SO_4^{2-} group was indicated by the appearance of ν_3(S—O) bands at 1167 and 1019 cm^{-1} which are characteristic for the high symmetry T_d (tetrahedral) point group [18,34]. In complex **4**, the broad band around 1089 cm^{-1} assigned to ν_3(Cl—O) indicates the noncoordinated (ionic) nature of the ClO_4^- ion [35,36] (T_d symmetry). The ionic nature is further supported by the appearance of a band at 625 cm^{-1} [35,37]. Support for the

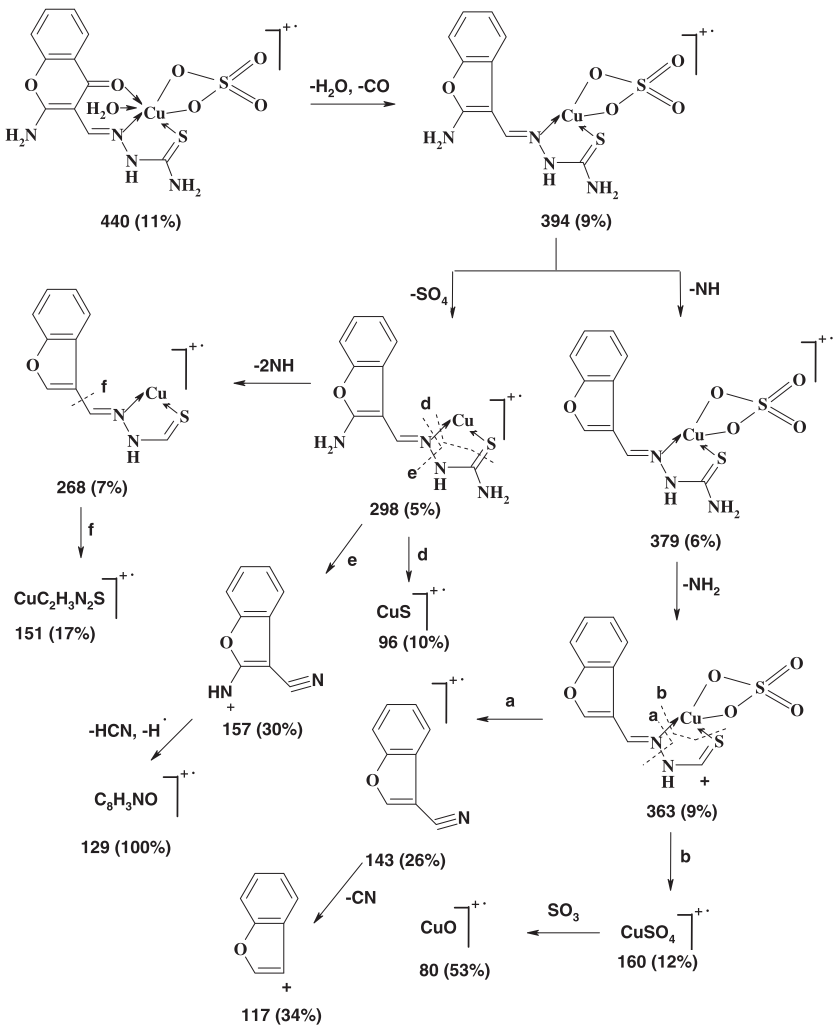

Scheme 4. Mass fragmentation pattern of complex **3**, [(HL)Cu(SO_4)(H_2O)].

above interpretation is the appearance of the non-ligand bands at 470–522 and 430–447 cm^{-1} assigned to ν(M—O) and ν(M—N) [38–40], respectively.

Conductivity measurements

The molar conductance values of the complexes in DMF (10^{-3} M solutions) were measured at room temperature and the results are listed in Table 3. The values showed that all complexes have non-electrolytic nature except complexes (**4** and **6**) which gave molar conductance value = 130 and 105 Ω^{-1} cm^2 mol^{-1}, suggesting their 1:2 and 1:1 electrolytic nature, respectively. This is consistent with the infrared data. In case of complexes **3**, **5** and **8**, the relatively high values of the molar conductance data may be due to the partial dissociation in their DMF solutions, however, they did not reach the previously reported values for 1:1 electrolytes in DMF solutions (~70–110) Ω^{-1} cm^2 mol^{-1} [41].

Magnetic measurements and electronic spectra

Due to the Jahn–Teller distortion and because of the low symmetry of the environment around Cu^{II}-ion (d^9), detailed interpretations of the spectra and magnetic properties are somewhat complicated [42]. The magnetic moment values of the complexes are in the range 1.45–1.78 B.M., which is consistent with the presence of one unpaired electron [43,44]. The subnormal magnetic moment values may be due to anti-ferromagnetic exchange; the smallest μ_{eff} values, the strongest is the exchange [45–47]. The electronic spectra of the complexes (**1**, **3**, **4**, **7** and **8**) show two absorption bands in the ranges 455–486 and 578–665 nm which may be assigned to the $^2B_{1g} \rightarrow {}^2E_g$ and $^2B_{1g} \rightarrow {}^2B_{2g}$ transitions, respectively corresponding to a distorted octahedral geometry [38,48]. On the other hand, complexes (**2**, **5** and **6**) show one band in the range 573–582 nm, respectively, which may be assigned to the $^2B_{1g} \rightarrow {}^2A_{1g}$ transition in a square planar geometry [35,49–51].

EPR spectra

To obtain further information about the stereochemistry and the site of the metal ligand bonding, EPR spectra of the complexes (**4** and **7**) were recorded in the solid state. Fig. 1 represents the EPR spectra of these complexes. The shapes of the spectra are consistent with octahedral geometry around the Cu(II) center in the complexes [33,35,38]. The spin Hamiltonian parameters of the complexes were calculated and summarized in Table 6. The room temperature solid state EPR spectra of the complexes are quite similar and exhibit an axially *g*-tensor parameters with $g_{||} > g_{\perp} > 2.0023$. In axial symmetry, the *g*-values are related by the expression, $G = (g_{||}-2)/(g_{\perp}-2) = 4$, which measures the exchange interaction between copper centers in the solid. According to Hathaway [52,53], if the value of *G* is greater than four, the exchange interaction between copper(II) centers in the solid state is negligible, whereas when *G* is lower than 4, a considerable exchange

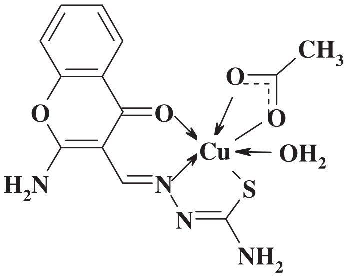

(1)

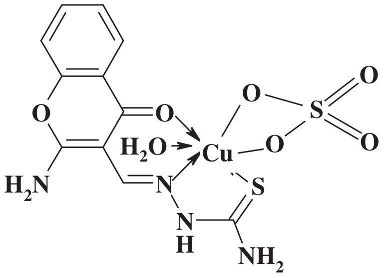

(3)

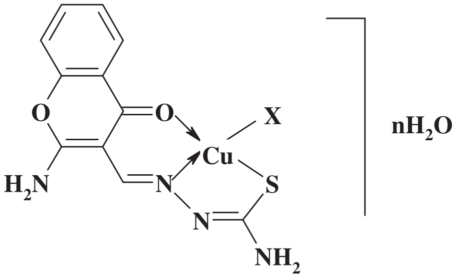

X	n	Complex
NO_3	nil	**2**
Cl	0.5	**5**

Fig. 3. Representative structures of the neutral complexes obtained by using AcO^-, SO_4^{2-}, NO_3^- and Cl^- anions.

interaction is indicated in the solid complex. The calculated *G* values (Table 6) are lower than four, suggesting copper–copper exchange interactions [29,54–56]. Molecular orbital coefficients, α^2(a measure of the covalency of the in-plane σ-bonding between a copper 3d orbital and the ligand orbitals) and β^2(covalent in-plane π-bonding), were calculated by using the following equations [57].

$$\alpha^2 = \left(\frac{A_{\parallel}}{0.036}\right) + (g_{\parallel} - 2.0023) + \frac{3}{7}(g_{\perp} - 2.0023) + 0.04, \beta^2 = -\frac{(g_{\parallel} - 2.0023)E}{8\lambda\alpha^2},$$

where $\lambda = -828\ \text{cm}^{-1}$ for the free copper ion and *E* is the electronic transition energy, $\alpha^2 = 1$ indicates complete ionic character, whereas $\alpha^2 = 0.5$ denotes 100% covalent bonding, with the assumption of negligibly small values of the overlap integral. The lower values of α^2(0.60–0.61) compared to β^2(0.76–0.83) indicate that the in-plane σ-bonding is more covalent than the in-plane π-bonding. These data are in good agreement with the data reported earlier [58–61].

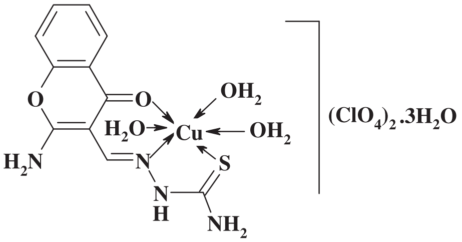

(4)

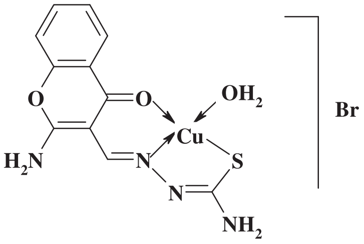

(6)

Fig. 4. Representative structures of the cationic complexes obtained by using ClO_4^- and Br^- anions.

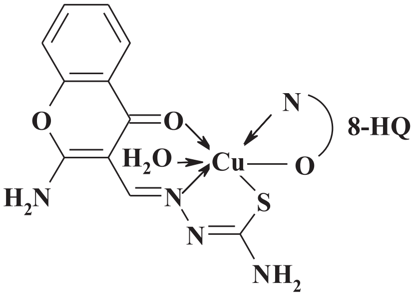

(7)

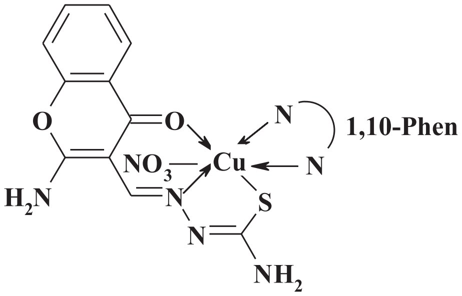

(8)

Fig. 5. Representative structures of the ternary complexes.

Thermal analysis

Thermal gravimetric analysis (TGA) was mainly used to proof the associated water or solvent molecules to be in the coordination sphere or in the outer sphere of the complex [49]. Complexes **2**, **3** and **5** were taken as representative examples for thermal analysis. The results of thermal analysis of these complexes are in agreement with elemental analyses.

The thermogram of complex (**3**), $[(HL)Cu(SO_4)(H_2O)]$, showed a weight loss in the range 33–144 °C which corresponds to one coordinated water molecule (weight loss; Calc./Found%; 4.09/4.03%). In case of complex **5**, $[(L)CuCl(H_2O)]\cdot 0.5H_2O$, the weight loss in the range 30–105 °C corresponds to half non-coordinated water molecule (weight loss; Calc./Found%; 2.44/2.24%). However, the

Table 7
Antimicrobial activity of the ligand and its Cu(II) complexes.

Organism	Mean of zone diameter, nearest whole[a] (mm)											
	Gram-positive bacteria				Gram-negative bacteria				Yeasts and Fungi[b]			
	Staphylococcus aureus (ATCC 25923)		*Bacillus subtilis* (ATCC 6635)		*Salmonella typhimurium* (ATCC 14028)		*Escherichia coli* (ATCC 25922)		*Candida albicans* (ATCC 10231)		*Aspergillus fumigatus*	
	Concentration											
Sample	1 mg/ml	0.5 mg/ml	1 mg/ml	0.5 mg/ml	1 mg/ml	0.5 mg/ml	1 mg/ml	0.5 mg/ml	1 mg/ml	0.5 mg/ml	1 mg/ml	0.5 mg/ml
HL	3 L	2 L	4 L	–	3 L	–	4 L	–	5 L	–	3 L	1 L
[(L)Cu(OAc)(H_2O)] (**1**)	–	–	7 L	2 L	9 L	8 L	–	–	–	–	–	–
[(L)Cu(NO_3)] (**2**)	4 L	–	8 L	4 L	14 I	9 I	4 L	–	14 I	11 I	3 L	–
[(HL)Cu(SO_4)(H_2O)] (**3**)	8 L	5 L	16 I	10 I	9 L	7 L	–	–	7 L	6 L	–	–
[(HL)Cu(H_2O)$_3$](ClO_4)$_2$·3H_2O (**4**)	6 L	4 L	25 H	18 H	23 I	15 I	–	–	9 L	5 L	7 L	4 L
[(L)CuCl(H_2O)]·0.5H_2O (**5**)	12 L	7 L	21 I	15 I	17 I	15 I	9 L	5 L	20 I	14 I	7 L	3 L
[(L)Cu(H_2O)]Br (**6**)	8 L	6 L	16 I	11 I	20 I	12 I	10 L	6 L	8 L	5 L	6 L	4 L
[(L)Cu(8-HQ)(H_2O)] (**7**)	6 L	5 L	14 I	11 I	19 I	15 I	8 L	5 L	11 L	8 L	–	–
[(L)Cu(NO_3)(Phen)] (**8**)	–	–	7 L	3 L	–	–	–	–	8 L	4 L	–	–
Control[c]	35	26	35	25	36	28	38	27	35	28	37	26

– = No effect.
L: Low activity = Mean of zone diameter ⩽ 1/3 of mean zone diameter of control.
I: Intermediate activity = Mean of zone diameter ⩽ 2/3 of mean zone diameter of control.
H: High activity = Mean of zone diameter > 2/3 of mean zone diameter of control.
[a] Calculated from three values.
[b] Identified on the basis of routine cultural, morphological and microscopical characteristics.
[c] Chloramphenicol in the case of Gram-positive bacteria, cephalothin in the case of Gram-negative bacteria and cycloheximide in the case of fungi.

coordinated water molecule was lost during the subsequent decomposition stage of the complex. Finally, The thermogram of complex **2**; [(L)Cu(NO_3)] showed no weight loss up to 230 °C, indicating the absence of water molecules in this complex.

Mass spectra

The mass spectra of the complexes **1, 2, 3** and **8**, as representative complexes, provide good evidence for the molecular formulas of these complexes. Fig. 2 depicts the mass spectra of complexes **3** and **8**. The mass spectra of the complexes **1, 2, 3,** and **8** showed the highest mass peak with *m*/*z* 401, 386, 440 and 567, respectively which agree very well with the formula weights of the complexes [(L)Cu(OAc)(H_2O)] (F. Wt = 401.89), [(L)Cu(NO_3)] (F. Wt = 386.83), [(HL)Cu(SO_4)(H_2O)] (F. Wt = 439.91), and [(L)Cu(NO_3)(Phen)] (F. Wt = [567.05]). The fragmentation pattern of complex **3**, [(HL)Cu(SO_4)(H_2O)], is depicted in Scheme 4.

Finally, from the interpretation of elemental and thermal analyses and spectral data (infrared, electronic, EPR and mass) as well as conductivity and magnetic susceptibility measurements at room temperature, it is possible to draw up the tentative structures of the metal complexes. Figs. 3–5 represent the proposed structures of the metal complexes.

Antimicrobial studies

The antimicrobial activity of the ligand and its metal complexes was investigated against the sensitive organisms *S. aureus* (ATCC 25923) and *B. subtilis* (ATCC 6635) as Gram-positive bacteria, *E. coli* (ATCC 25922) and *S. typhimurium* (ATCC 14028) as Gram-negative bacteria, yeast: *C. albicans* (ATCC 10231) and fungus: *A. fumigatus*. The results are listed in Table 7. Inspection of the data given in Table 7 reveals that the ligand and most of its metal complexes showed an antimicrobial activity. Generally, the complexes have higher activity than the organic ligand. A possible explanation for the observed increased activity upon chelation is that the positive charge of the metal in chelated complex is partially shared with the ligand's donor atoms so that there is an electron delocalization over the whole chelate ring. This, in turn, will increase the lipophilic character of the metal [62,63]. Complex **5**, [(L)CuCl(H_2O)]·0.5H_2O, showed the highest activity towards the Gram-positive bacteria (*S. aureus*) and towards yeast *C. albicans* while complex **4**, [(HL)Cu(H_2O)$_3$](ClO_4)$_2$·3H_2O showed the highest activity towards the Gram-positive bacteria (*B. subtilis*), the Gram-negative bacteria (*S. typhimurium*) and *A. fumigatus*. On the other hand, complex **6**, [(L)Cu(H_2O)]Br showed the highest activity towards the Gram-negative bacteria (*E. coli*). Finally, complexes **4** and **5** seem to be promising since they showed antimicrobial activity comparable to those of chloramphenicol, cephalothin and cycloheximide.

Conclusion

The condensation reaction of 2-aminochromone-3-carboxaldehyde with thiosemicarbazide afforded the tridentate thiosemicarbazone, HL, ligand. The reactions of the ligand with different copper(II) salts afforded neutral and cationic mononuclear complexes. The spectroscopic data showed that the ligand acts as neutral or monobasic tridentate ligand through the γ-pyrone oxygen, azomethine nitrogen and the thionic/thiolic sulfur. The metal complexes exhibited octahedral and square planar geometrical arrangements. The ligand and some complexes showed antimicrobial activity.

References

[1] L.-J. Ming, Med. Res. Rev. 23 (2003) 697–762.
[2] T.S. Lobana, R. Sharma, G. Bawa, S. Khanna, Coord. Chem. Rev. 253 (2009) 977–1055.
[3] A. Sankaraperumal, J. Karthikeyan, A.N. Shetty, R. Lakshmisundaram, Polyhedron 50 (2013) 264–269.
[4] W. Yu, L. Shi, G. Hui, F. Cui, J. Lumines. 134 (2013) 491–497.
[5] T.A. Yousef, G.M. Abu El-Reash, O.A. El-Gammal, R.A. Bedier, J. Mol. Struct. 1029 (2012) 149–160.
[6] E. Ramachandran, D. Senthil Raja, N.S.P. Bhuvanesh, K. Natarajan, Dalton Trans. 41 (2012) 13308–13323.
[7] R.J. Glisoni, M.L. Cuestas, V.L. Mathet, J.R. Oubina, A.G. Moglioni, A. Sosnik, Eur. J. Pharm. Sci. 47 (2012) 596–603.
[8] I.C. Mendes, F.B. Costa, G.M. de Lima, J.D. Ardisson, I. Garcia-Santos, A. Castiñeiras, H. Beraldo, Polyhedron 28 (2009) 1179–1185.
[9] D. Kovala-Demertzi, A. Papageorgiou, L. Papathanasis, A. Alexandratos, P. Dalezis, J.R. Miller, M.A. Demertzis, Eur. J. Med. Chem. 44 (2009) 1296–1302.

[10] J. Lu, H. Guo, X. Zeng, Y. Zhang, P. Zhao, J. Jiang, L. Zang, J. Inorg. Biochem. 112 (2012) 39–48.
[11] M. Padmaja, J. Pragathi, B. Anupama, C.G. Kumari, E-J. Chem. 9 (2012) 2145–2154.
[12] Y. Li, Z.-Y. Yang, T.-R. Li, Z.-C. Liu, B.-D. Wang, J. Fluoresc. 21 (2011) 1091–1102.
[13] T.E. Ali, M.A. Ibrahim, J. Braz. Chem. Soc. 21 (2010) 1007–1016.
[14] Y. Li, Z.-Y. Yang, J. Fluoresc. 20 (2010) 329–342.
[15] T. Walenzyk, C. Carola, H. Buchholz, B. König, Tetrahedron 61 (2005) 7366–7377.
[16] V. Arjunan, S. Subramanian, S. Mohan, Spectrochim. Acta A 60 (2004) 995–1000.
[17] O.E. Sherif, H.M. Abd El-Fattah, M.M. El-Ajily, J. Therm. Anal. Calorim. 74 (2003) 181–200.
[18] M. Shebl, H.S. Seleem, B.A. El-Shetary, Spectrochim. Acta A 75 (2010) 428–436.
[19] S.M.E. Khalil, M. Shebl, F.S. Al-Gohani, Acta Chim. Slov. 57 (2010) 716–725.
[20] H.S. Seleem, B.A. El-Shetary, S.M.E. Khalil, M. Mostafa, M. Shebl, J. Coord. Chem. 58 (2005) 479–493.
[21] H.S. Seleem, A.A. Emara, M. Shebl, J. Coord. Chem. 58 (2005) 1003–1019.
[22] A. Nohara, T. Umetani, Y. Sanno, Tetrahedron 30 (1974) 3553–3561.
[23] U. Petersen, H. Heitzer, Liebigs Ann. Chem. 9 (1976) 1659–1662.
[24] M.A. Ibrahim, K.M. El-Mahdy, Phosphorus, Sulfur, Silicon Relat. Elem. 184 (2009) 2945–2954.
[25] F.E. Mabbs, D.I. Machin, Magnetism and Transition Metal Complexes, Chapman and Hall, London, 1973.
[26] A.U. Rahman, M.I. Choudhary, W.J. Thomsen, Bioassay Techniques for Drug Development, Harwood Academic Publishers, The Netherlands, 2001.
[27] K.M. Khan, Z.S. Saify, A.K. Zeesha, M. Ahmed, M. Saeed, M. Schick, H.J. Kohlbau, W. Voelter, Arzneim. Forsch. 50 (2000) 915–922.
[28] A.A. El-Asmy, O.A. El-Gammal, H.S. Saleh, Spectrochim. Acta A 71 (2008) 39–44.
[29] A.A. El-Asmy, M.A. Abdallah, Sh.A. Mandour, K.M. Ibrahim, Synth. React. Inorg. Met.-Org. Nano-Met. Chem. 40 (2010) 675–689.
[30] M.S. Refat, I.M. El-Deen, Z.M. Anwer, S. El-Ghol, J. Mol. Struct. 920 (2009) 149–162.
[31] S.A. Khan, M. Yusuf, Eur. J. Med. Chem. 44 (2009) 2270–2274.
[32] M. Shebl, S.M.E. Khalil, A. Taha, M.A.N. Mahdi, J. Am. Sci. 8 (2012) 183–197.
[33] M. Shebl, Spectrochim. Acta A 73 (2009) 313–323.
[34] S.M.E. Khalil, K.A. Bashir, J. Coord. Chem. 55 (2002) 681–696.
[35] M. Shebl, Spectrochim. Acta A 70 (2008) 850–859.
[36] L.M. Fostiak, I. García, J.K. Swearingen, E. Bermejo, A. Castiñeiras, D.X. West, Polyhedron 22 (2003) 83–92.
[37] A. Taha, Spectrochim. Acta A 59 (2003) 1611–1620.
[38] M. Shebl, J. Coord. Chem. 62 (2009) 3217–3231.
[39] M. Shebl, S.M.E. Khalil, A. Taha, M.A.N. Mahdi, J. Mol. Struct. 1027 (2012) 140–149.
[40] S.M.E. Khalil, H.S. Seleem, B.A. El-Shetary, M. Shebl, J. Coord. Chem. 55 (2002) 883–899.
[41] W.J. Geary, Coord. Chem. Rev. 7 (1971) 81–112.
[42] F.A. Cotton, G. Wilkinson, Advanced Inorganic Chemistry, fourth ed., John Wiley and Sons, New York, 1980.
[43] M. Shebl, S.M.E. Khalil, F.S. Al-Gohani, J. Mol. Struct. 980 (2010) 78–87.
[44] H.S. Seleem, B.A. El-Shetary, M. Shebl, Heteroatom. Chem. 18 (2007) 100–107.
[45] O. Khan, Molecular Magnetism, VCH, New York, 1993.
[46] S.S. Massoud, F.A. Mautner, R. Vicente, J.S. Dickens, Inorg. Chim. Acta 361 (2008) 299–308.
[47] C.J. Jones, d- and f- Block Chemistry, Polestar Wheatones Ltd., UK, 2001.
[48] M.M. Mashaly, Z.H. Abd El-Wahab, A.A. Faheim, J. Chin. Chem. Soc. 51 (2004) 1–15.
[49] M. Shebl, S.M.E. Khalil, S.A. Ahmed, H.A.A. Medien, J. Mol. Struct. 980 (2010) 39–50.
[50] S. Chandra, X. Sangeetika, Spectrochim. Acta A 60 (2004) 147–153.
[51] R. Atkins, G. Brewer, E. Kokot, G.M. Mocler, E. Sinn, Inorg. Chem. 24 (1985) 127–134.
[52] B.J. Hathaway, D.E. Billing, Coord. Chem. Rev. 5 (1970) 143–207.
[53] B.J. Hathaway, Struct. Bond. 57 (1984) 55–118.
[54] A.A. El-Asmy, G.A.A. Al-Hazmi, Spectrochim. Acta A 71 (2009) 1885–1890.
[55] S.O. Bahaffi, A.A. Abdel Aziz, M.M. El-Naggar, J. Mol. Struct. 1020 (2012) 188–196.
[56] A.A. El-Asmy, J. Sulfur Chem. 30 (2009) 64–73.
[57] C.J. Carrano, C.M. Nunn, R. Quan, J.A. Bonadies, V.L. Pecoraro, Inorg. Chem. 29 (1990) 944–951.
[58] N.M. El-Metwally, A.A. El-Asmy, J. Coord. Chem. 59 (2006) 1591–1601.
[59] G.A.A. Al-Hazmi, M.S. El-Shahawi, I.M. Gabr, A.A. El-Asmy, J. Coord. Chem. 58 (2005) 713–733.
[60] U. El-Ayaan, I.M. Gabr, Spectrochim. Acta A 67 (2007) 263–272.
[61] M. Shebl, S.M.E. Khalil, A. Taha, M.A.N. Mahdi, Spectrochim. Acta A 113 (2013) 356–366.
[62] N. Fahmi, I.J. Gupta, R.V. Singh, Phosphorus, Sulfur, Silicon Relat. Elem. 132 (1998) 1–8.
[63] A. Chaudhary, R.V. Singh, Phosphorus, Sulfur, Silicon Relat. Elem. 178 (2003) 603–613.